scientific reports

Check for updates

OPEN

Effect of 660-nm LED photobiomodulation on the proliferation and chondrogenesis of meniscus-derived stem cells (MeSCs)

Jiabei Tong[1,2]✉, Suresh Kumar Subbiah[3], Sanjiv Rampal[4,5], Rajesh Ramasamy[6], Xiaoyun Wu[7], Yanyan You[8], Jiaojiao Wang[9] & Pooi Ling Mok[1]✉

Meniscus-derived stem cells (MeSCs), a unique type of MSC, have outstanding advantages in meniscal cytotherapy and tissue engineering, but the effects and molecular mechanisms of PBM on MeSCs are still unclear. We used 660-nm LED light with different energy densities to irradiate six human MeSC samples and tested their proliferation rate via cell counting, chondrogenic differentiation capacity via the DMMB assay, mitochondrial activity via the MTT assay, and gene expression via qPCR. The proliferation ability, chondrogenic capacity and mitochondrial activity of the 18 J/cm^2 group were greater than those of the 4 J/cm^2 and control groups. The mRNA expression levels of *Akt*, *PI3K*, *TGF-β3*, *Ki67* and *Notch-1* in the 18 J/cm^2 group were greater than those in the other groups in most samples. After chondrogenic induction, the expression of *Col2A1*, *Sox9* and *Aggrecan* in the 18 J/cm^2 group was significantly greater than that in the 4 J/cm^2 and control groups in most of the samples. The variation in the MTT values and *Src*, *PI3K*, *Akt*, *mTOR* and *GSK3β* levels decreased with time. The results showed that 660-nm LED red light promoted proliferation and chondrogenic differentiation and affected the gene expression of MeSCs, and the effects on gene expression and mitochondrial activity decreased with time.

The knee meniscus, a vital tissue responsible for load transmission and shock absorption in the knee joint, is prone to injury and has limited self-repair capabilities. Progressive deterioration of meniscal injuries often leads to cartilage wear and eventually degenerative knee disease, osteoarthritis and, in some individuals, total knee replacement surgery[1,2]. The prevalence of meniscal injuries is particularly high among the middle-aged and elderly population, with an increasing trend observed in young adults[1,3]. Surgery is by far the most common medical intervention for meniscal injuries, but the success rate of treatment is low[4]. Most patients experience aggravated injuries leading to meniscectomy and osteoarthritis, resulting in missed work and a significant financial burden[4].

[1]Department of Biomedical Science, Faculty of Medicine and Health Sciences, Universiti Putra Malaysia, 43400 Serdang, Selangor, Malaysia. [2]The Fifth People's Hospital of Luoyang (The Fifth Affiliated Hospital of Henan University of Science and Technology), No.505 Taikang East Road, Luolong District, Luoyang City 471000, Henan Province, China. [3]Center for Global Health Research, Saveetha Medical College and Hospitals, Saveetha Institute of Medical and Technical Sciences, Chennai, Tamil Nadu 602105, India. [4]Orthopaedic Department, School of Medicine, International Medical University, 57000 Kuala Lumpur, Malaysia. [5]Department of Orthopaedic and Traumatology, Faculty of Medicine and Health Sciences, Universiti Putra Malaysia, 43400 Serdang, Selangor, Malaysia. [6]Department of Pathology, Faculty of Medicine and Health Sciences, Universiti Putra Malaysia, 43400 Serdang, Selangor, Malaysia. [7]Department of Technology, Inner Mongolia Stem Cell (ProterCell) Biotechnology Co., Ltd., Hohhot, China. [8]Pharmacy Department, Tongliao Hospital, Tongliao 028000, Inner Mongolia, China. [9]Department of Obstetrics and Gynecology, Maternal and Child Health Hospital of Haidian District, Beijing 100080, China. ✉email: hanfabin1@gmail.com; pooi_ling@upm.edu.my

Regenerative medicine repair using stem cells holds great promise for meniscal repair, with research focusing on injectable treatments and tissue engineering using mesenchymal stem cells (MSCs)[5,6]. MeSCs display many characteristics very similar to those of MSCs, including cell surface markers ($CD14^+$, $CD29^+$, $CD44^+$, $CD73^+$, $CD90^+$, $CD105^+$, $CD34^-$, and $CD45^-$) and osteogenic, adipogenic and chondrogenic differentiation capacities[7,8]. MeSCs are ideal cells for meniscal cytotherapy and meniscal tissue engineering because of their advantages in terms of chondrogenic differentiation potential, easy access to cell sources, and high adaptability to the microenvironment of the meniscal tissue[7,9].

Photobiomodulation (PBM) is a noninvasive therapy that uses a low-intensity light-emitting diode (LED), laser or broadband light to relieve pain, reduce inflammation, and enhance healing; thus, it has been used clinically to promote wound healing in various tissues[10–12]. Numerous studies have shown that PBM can affect the proliferation, differentiation and migration of MSCs in vitro[13]. We hope that these similar or better effects on MeSCs can be used as an ideal pretreatment for meniscal cell therapy and tissue engineering in the future.

PBM is also a potential means to enhance the performance of MSCs in tissue engineering materials and has been demonstrated in tissue engineering studies in a variety of tissues[14,15]. Red light (600–700 nm) easily penetrates tissues, especially collagen and other substances in tissues, so it is widely used in clinical and experimental applications and is suitable for promoting cartilage and other types of tissue repair[14,15]. Several in vitro studies have demonstrated its ability to promote cell proliferation[16], differentiation[17], and migration[18]. Although many studies have been published on the effects of PBM on MSCs, many of them lack in-depth investigations on the related gene expression and molecular mechanisms. In recent years, some studies on the differentiation capacity of dental pulp stem cells have detected cytochemical changes only by staining, not by measuring RNA and protein levels[19,20]. Other studies on the cartilage differentiation of bone marrow MSCs have detected only the expression of genes related to cartilage differentiation products but not the expression of genes upstream of the cartilage differentiation pathway, which is directly related to PBM[21].

In our unpublished study, we isolated, cultured and characterized MeSCs from six osteoarthritis patients. The characterization results revealed that these cells exhibited an MSC-specific phenotype and multilineage differentiation ability in vitro. The MeSCs expressed high levels of CD29, CD44, CD73, CD90 and CD105 but not the hematopoietic markers CD34 and CD45. After a 4-week culture period of adipogenic differentiation induction, most cells exhibited positive Oil Red O staining, indicating adipogenic differentiation. Upon osteogenic differentiation induction, all the cell populations produced a mineralized matrix, as confirmed by Alizarin Red staining. When cultured in chondrogenic medium, all the cells presented glycosaminoglycan (GAG) deposition, as evidenced by Alcian blue staining. These characteristics are consistent with those previously reported for MeSCs[7,22,23].

In a previous study, we compared the differences in the proliferative capacity, differentiation potential, cell phenotype and gene expression of cells with different media compositions and different numbers of media. We found that cells cultured in low-glucose DMEM as the basal medium supplemented with fetal bovine serum (FBS) and fibroblast growth Factor 2 (FGF2) cytokines presented increased proliferative capacity and chondrogenic differentiation ability (unpublished data). To investigate the mechanism of the changes in the chondrogenic differentiation potential of MeSCs, we cultured the cells in the optimized culture medium and irradiated them with 660 nm LED PBM.

Methods

In the present study, the medial and lateral meniscuses of human patients who underwent total knee arthroplasty at Hospital Sultan Abdul Aziz Shah, Universiti Putra Malaysia, were obtained with the approval of the Ethics Committee for Research Involving Human Subject-Universiti Putra Malaysia Malaysia (Ethics approval No. JKEUPM-2020-26). The donors consisted of three females and three males (mean age: 68 ± 2.5; age range: 66–72 years). The meniscus tissues were rinsed five times with phosphate-buffered saline and immersed in a 5% solution of penicillin−streptomycin (Life Technologies, Carlsbad, CA) for 15 min. Then, the meniscus tissues were treated with collagenase type I (2 mg/ml; Solarbio, Beijing, China) in DMEM/F12 (Nacalai Tesque, San Diego, CA, USA) and 1% penicillin−streptomycin F12 (Nacalai Tesque, San Diego, CA, USA) for 6 h. The digested tissues were subsequently passed through 70-μm cell strainers (Millipore Sigma, St. Louis, MO, USA) and then cultured in DMEM/F12 F12 (Nacalai Tesque, San Diego, CA, USA) supplemented with 10% fetal calf serum (FBS) (Sigma, St. Louis, MO, USA) and 1% penicillin−streptomycin (Nacalai Tesque, San Diego, CA, USA). The cells (P0) were grown until they reached a density of 80% confluence before being split into new flasks. The cell samples used in the downstream experiments were labeled with Nos. 1 to 6. The surface phenotypes of the cells were tested via flow cytometry, and their capacity to differentiate into adipogenic, osteogenic and chondrogenic lineages was determined. The results confirmed the similarities in their characteristics with those of mesenchymal stem cells (unpublished data) and were in agreement with those of other studies[22–24].

Cell irradiation

MeSCs that were isolated and identified in previous studies were used in this study. The cells were then cultured in medium composed of DMEM (LG) (Nacalai Tesque, San Diego, CA, USA), 10% fetal bovine serum (FBS) (Sigma, St. Louis, MO, USA), 1% penicillin/streptomycin, 2 mM GlutaMAX (Solarbio, Beijing, China), and 2 ng/mL basic fibroblast growth factor (FGF2; Sigma, St. Louis, MO, USA) inside a humidified incubator (37 °C, 5% CO_2). The passage 2 cells were harvested and then seeded into a 35-mm petri dish and grown to 80% confluence. The current initial study with PBM irradiation aimed to investigate the effects of PBM on cell proliferation, chondrogenic induction, mitochondrial activity and gene expression. The cells were grouped according to the 0 J/cm^2, 4 J/cm^2 and 18 J/cm^2 energy densities and irradiated at 24-h intervals for a total of three irradiations. Meanwhile, to identify the specific gene changes in the cells (*JNK*, *p38*, *MARK*, *JAK*, *Bax*, *Bcl2*, *Akt-1*, *PI3K*, *Src*,

GSK3β, *mTOR*, *p53* and *p21*) following introduction to PBM, MeSCs from donor No. 1 were irradiated once at 18 J/cm^2, and gene expression assays were performed at 8, 16 and 24 h after irradiation. To assess whether the cells would exhibit greater mitochondrial activity at higher energy densities, we also irradiated the MeSCs once at 18 J/cm^2 and 30 J/cm^2 and assessed their mitochondrial activity via the MTT assay.

The light source for cell irradiation used in the current study was an LH-SDT5W red light therapy device (Lv Heng Sdn Bhd, Shenzhen, Guangdong, China). The output power at the material irradiation distance was determined with an SM206 photo power meter (Xin Bao Sdn Bhd, Shenzhen, Guangdong, China). The MeSCs were cultured in a 35-mm petri dish. The LED light source was maintained at a distance of 15 mm from the cells for irradiation, and the spot size was 35 mm in diameter (Fig. 1). A power meter was used to determine the energy output in the area of light exposure, and the power density was measured to be 35.398 W/cm^2. The culture medium was removed just before cell irradiation. To irradiate the cells with energy densities of 4 J/cm^2, 18 J/cm^2 and 30 J/cm^2, the cells were irradiated in the dark for 113 s, 508 s, and 847.5 s, respectively. Irradiation was performed at room temperature. In the control group, the cells were not irradiated. New culture medium was added to the cells immediately after irradiation.

Energy density was calculated via the following formula: energy density (J/cm^2) = power density (W/cm^2) × irradiation time (seconds).

Cell propagation

To evaluate the changes in the proliferative capacity of MeSCs after irradiation, a uniform population of 1500 viable cells per cm^2 was seeded on 6-well cell culture plates. The cells were then cultured in the same environment as described above.The culture medium was completely replaced 24 h after the initial seeding and every 3 days thereafter. The resulting cells were then plated at the original seeding density every 10 days.

To determine the proliferation potential of MeSCs, the cells harvested at the end of each passage were counted via the trypan blue exclusion method. The number of cells that doubled (NCPD) and the cell population doubling time (CPDT) were subsequently calculated via the following formulas[25]:

$$\mathrm{NCPD} = 3.33 * \log\left(N_t/N_i\right);$$

$$\mathrm{CPDT} = (t - t_i) * \log\{2 * \log(N_t/N_i)\}^{-1}.$$

where N_t and N_i are the cell numbers at a specific time point t (Day 10) and at initial seeding (Day 0), respectively.

MTT assay

After irradiation, formazan production was measured via MTT. Formazan production is related to mitochondrial metabolic activity. The cells were seeded in a 96-well plate at 5000 cells/well in a 100-µL volume and incubated overnight at 37 °C with 5% CO_2. A solution containing 0.5 mg/mL 3-(4,5-dimethyl-2-thiazolyl)-2,5-diphenyl-2H-tetrazolium bromide (MTT; Solarbio, Beijing, China) was added to the wells, and the plates were incubated at 37 °C for 4 h in the dark. DMEM containing MTT was then removed from the wells, and dimethyl sulfoxide (DMSO, Solarbio, Beijing, China) was added to solubilize the formed crystals. Formazan formation was measured spectrophotometrically (Flx 800 Fluorescence Microplate Reader; Agilent, CA, USA) at 570 and 630 nm, and the net ΔA (570–630) nm was used as an index of mitochondrial function. The results are expressed as a percentage of the control, which was assigned 100% activity.

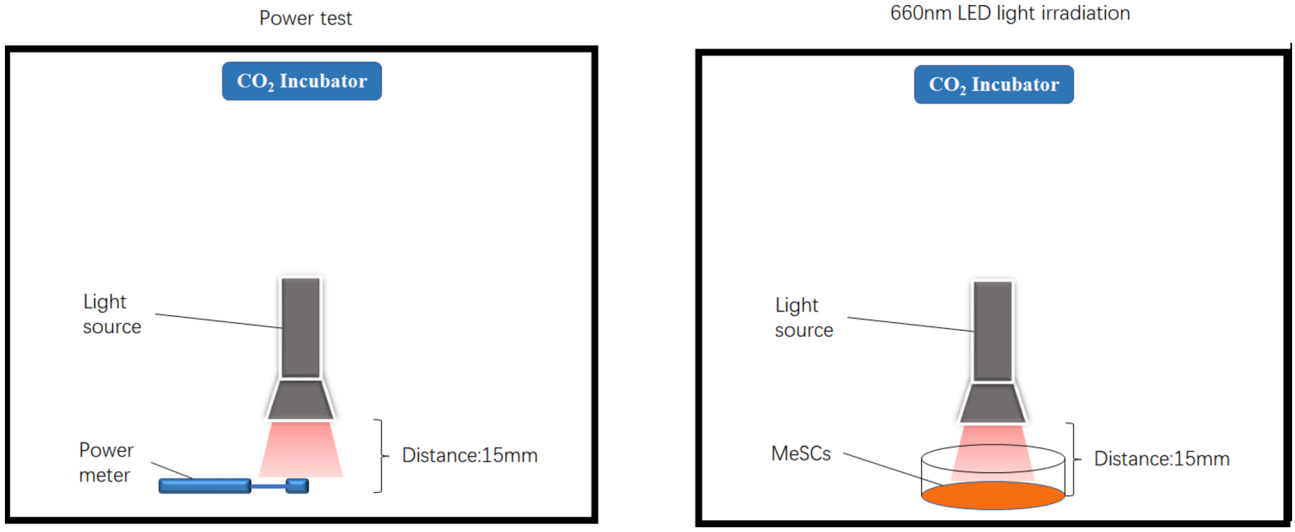

Figure 1. The MeSCs were expanded in cell culture flasks until passage 3. The energy output in the area of light exposure was measured with a power meter.

MeSC chondrogenic differentiation, the DMMB assay and Alcian blue staining

MeSCs were immediately exposed to chondrogenic conditions 24 h after irradiation to assess the chondrogenic differentiation potential. The chondrogenic differentiation medium used in this study was the MesenCult™-ACF Chondrogenic Differentiation Kit (05457), which was purchased from STEM CELL (Vancouver, BC, Canada).

Proteoglycan content was estimated by measuring glycosaminoglycan (GAG) content via a 1,9-dimethyl methylene blue (DMMB; Solarbio, Beijing, China) dye binding assay to assess the potential for chondrogenic differentiation. Specifically, a 20-μL sample was mixed with 200 μL of DMMB solution, and the absorbance was measured at a wavelength of 530 nm. A standard curve was generated using shark-derived chondroitin-6-sulfate (Solarbio, Beijing, China) to compare the absorbances of the samples.

After chondrogenic differentiation was induced, the cells were stained with Alcian blue solution (C0153S-1; Beyotime, Beijing, China). After the culture medium was removed, the cell-seeded hydrogels were fixed in 4% paraformaldehyde for 30 min and then washed three times with PBS before the addition of Alcian blue solution. After 30 min of incubation at room temperature, the dye solution was removed, and the constructs were washed with distilled water. The staining results were recorded under an inverted microscope.

Real-time PCR

The gene expression profiles of passaged MeSCs and differentiated cells were assessed via real-time polymerase chain reaction (qPCR). The cells were irradiated at 0, 4 or 18 J/cm^2 three times and harvested 24 h after the last irradiation. The cells from donor No. 1, which were irradiated once at 18 J/cm^2, were harvested at 8, 16 and 24 h after irradiation. Total RNA was extracted from the harvested cells via the Manual innuPREP DNA RNA Mini Kit 2.0, which was purchased from IST Innuscreen GmbH (Berlin, Germany). The RNA samples were then reverse transcribed into cDNA via the LunaScript® RT SuperMix Kit (New England Biolabs, MA, USA), and the resulting cDNA gene expression analysis was performed via TransStart® Tip Green qPCR SuperMix (TransGen Biotech, Beijing, China) according to the manufacturer's instructions. Each PCR was performed in technical triplicate for 40 cycles on a LightCycler® 480 Real-Time PCR System (Roche, IN, USA). The experiment began with 5 min of enzyme activation at 95 °C, followed by 40 cycles of 5 s at 95 °C and 30 s at 57 °C. The cycle threshold (Ct) value for each sample was determined by averaging triplicate measurements. A relative quantification method was used to analyze the data, where the fluorescence signals were adjusted relative to the expression of *β-actin* as a housekeeping gene. The primer sequences of the selected genes are listed in Table 1.

Statistical analysis

The data are presented as the mean ± SEM. Student's t test was used for comparisons between groups, where appropriate, via SPSS 27 (IBM, Chicago, IL, US). $p < 0.05$ was considered statistically significant.

Ethical approval

All the human sample isolation procedures were performed following the Guidelines of the National and International Ethical Guidelines for Biomedical Research Involving Human Subjects (CIOMS) and the Guideline for Stem Cell Research & Therapy, and they were approved by the Ethics Committee for Research Involving Human

Primers	forward	reverse
Human *Akt-1*	5′- TGAGACCGACACCAGGTATTTTG-3′	5′- GCTGAGTAGGAGAACTGGGGAAA-3′
Human *PI3K*	5′-CTGGAAGCCATTGAGAAG-3′	5′-CAGGATTTGGTAAGTCGG-3′
Human *Ki67*	5′-CTTCCAGCAGCAAATCTCA-3′	5′-ACAATCAGATTTGCTTCCGA-3′
Human *Notch-1*	5′-GTCCCACCCATGACCACTAC-3′	5′-CCTGAAGCACTGGAAAGGAC-3′
Human *Col2A1*	5′-CTCCTGGAGCATCTGGAGAC-3′	5′-ACCACGATCACCCTTGACTC-3′
Human *Sox9*	5′-CAGGCTTTGCGATTTAAGGA-3′	5′-CCGTTTTAAGGCTCAAGGTG-3′
Human *Aggrecan*	5′-CAACTACCCGGCCATCC-3′	5′-GATGGCTCTGTAATGGAACAC-3′
Human *TGF-β3*	5′-CTTTGGACACAAATTACTGCTTC-3′	5′- GGGTTCAGAGTGTTGTACAGTCC-3′
Human *JNK*	5′- AACTCTTTGACGCTGCTTGC-3′	5′- TGAAGCACTGTGCCTTTACC-3′
Human *p38*	5′- GAGCGTTACCAGAACCTGTCTC-3′	5′-AGTAACCGCAGTTCTCTGTAGGT-3′
Human *MAPK*	5′- AGCCCAAGGGATTGTTTGTG -3′	5′- AGGACGAGTTCACGATAAGCTC-3′
Human *JAK-1*	5′-GAGACAGGTCTCCCACAAACAC-3′	5′-GTGGTAAGGACATCGCTTTTCCG-3′
Human *SRC*	5′-CAATGCAAGGGCCTAAATGT-3′	5′-TGTTTGGAGTAGTAAGCCACGA-3′
Human *GSK3β*	5′-CCGACTAACACCACTGGAAGCT-3′	5′-AGGATGGTAGCCAGAGGTGGAT-3′
Human *mTOR*	5′-ACCCATCCAACCTGATGCTG-3′	5′-ACACTGTCCTTGTGCTCTCG-3′
Human *BAX*	5′-CGGCGAATTGGAGATGAACTGG-3′	5′-CTAGCAAAGTAGAAGAGGGCAACC-3′
Human *Bcl2*	5′-TACTTAAAAAATACAACATCACA-3′	5′-GGAACACTTGATTCTGGTG-3′
Human *p53*	5′-CCCCTCCATCCTTTCTTCTC-3’	5′-ATGAGCCAGATCAGGGACTG-3′
Human *p21*	5′-AGGTGGACCTGGAGACTCTCAG -3′	5′-TCCTCTTGGAGAAGATCAGCCG-3′
Human *β-actin*	5′- CACCATTGGCAAGCGGTTC -3′	5′-AGGTCTTTGCGGATGTCCACGT-3′

Table 1. Sequences of primers used for qPCR.

Subject-Universiti Putra Malaysia Malaysia (Ethics approval No. JKEUPM-2020–26). Informed consent was obtained from all participants.

Results

18 J/cm² PBM promoted the proliferation of MeSCs

After irradiation, the MeSCs were subcultured every 10 days, and NCPD and CPDT were measured after each passage (Fig. 2). While MeSCs irradiated at 18 J/cm^2 showed superior proliferative capacity (higher NCPD and lower CPDT) at passage 3, there were no significant differences between the groups at passages 4 and 5 in the No. 1–5 samples in the NCPD and No. 1–6 samples in the CPDT. Only the NCPD of No. 6 was significantly different between the 18 J/cm^2 group and the other two experimental groups at passages 4 and 5.

PBM promoted the mitochondrial activity of MeSCs

After 24 h of exposure to 660-nm LED red light irradiation, the MTT assay revealed that the mean 570/630-nm absorbance of the 18 J/cm^2 group was significantly greater than that of the control group for all six samples, but that of only two samples in the 4 J/cm^2 group was significantly greater than that of the control group.

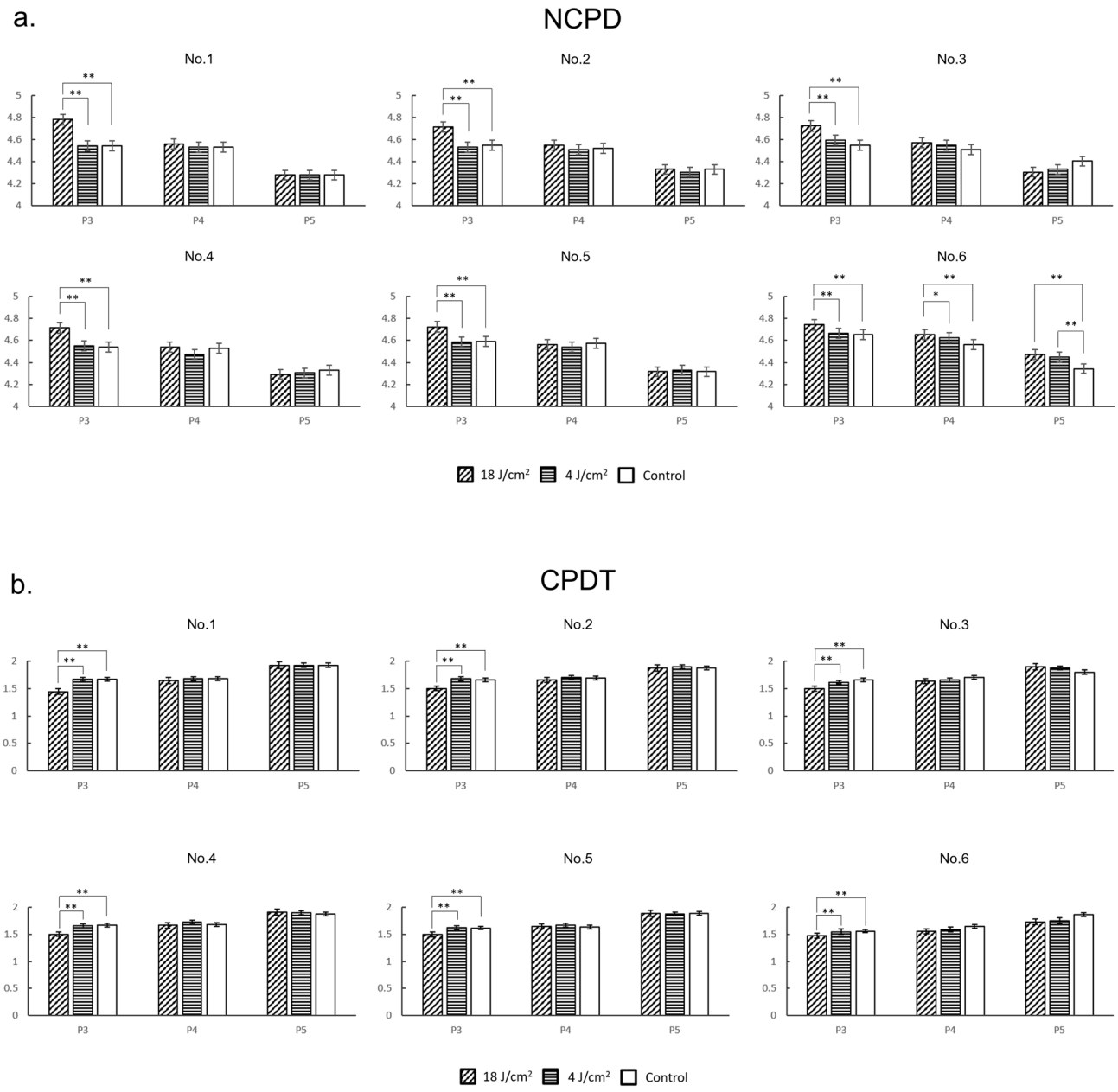

Figure 2. MeSCs were subcultured every 10 days, and NCPD and CPDT measurements were performed after each passage. Compared with those in the 4 J/cm^2 and control groups, the proliferative capacity of the MeSCs in the 18 J/cm^2 group was greater at passage 3. $n = 3$; $^*p < 0.05$, $^{**}p < 0.01$.

The absorbance at 570/630 nm was 17.0–72.4% greater in the 18 J/cm^2 group than in the control group and 12.8–18.0% greater in the 4 J/cm^2 group than in the control group (Fig. 3).

The MTT results after 18 and 30 J/cm^2 irradiation were significantly different from those of the control group ($p < 0.01$), 40.8–53.9% higher in the 18 J/cm^2 group than in the control group and 41.4–51.6% higher in the 30 J/cm^2 group than in the control group. There was no significant difference ($p > 0.05$) between the 18 and 30 J/cm^2 groups. At 24 h after irradiation, that of the 18 J/cm^2 group was 32.7–44.0% greater than that of the control group, and that of the 30 J/cm^2 group was 29.8–47.7% greater than that of the control group. There was no significant difference ($p > 0.05$) between the 18 and 30 J/cm^2 groups. When the MTT results at 4 and 24 h after irradiation were compared, the MTT values of the cells at 4 h were greater than those at 24 h, and the results were significantly different ($p < 0.05$). The energy density of 30 J/cm^2 did not improve the MTT detection value for MeSCs, and the MTT value decreased with time (Fig. 4).

PBM promoted the chondrogenic differentiation potential of MeSCs

DMMB assays were used to determine GAG production in differentiated MeSCs after irradiation (Fig. 5). After 28 days of chondrogenic induction in cells irradiated with 660-nm LED red light, the mean GAG concentration of the 18 and 4 J/cm^2 groups was significantly greater than that of the control group in all six samples, but no significant difference was found between the 18 and 4 J/cm^2 groups. The GAG concentration in the 18 J/cm^2 group was 37.2–44.2% greater than that in the control group, and the total mean GAG concentration in the 4 J/cm^2 group was 28.2–34.2% greater than that in the control group.

PBM affected the gene expression of the PI3K/Akt-related pathway in MeSCs

The expression of *Akt-1* (AKT serine/threonine kinase 1), *PI3K* (phosphatidylinositol-3-kinase), *Ki67* (proliferation marker Kiel 67), *Notch-1* (neurogenic locus notch homolog protein 1), *TGF-β3* (transforming growth factor beta 3), *Col2A1* (collagen type II alpha 1 chain), *Sox9* (SRY box transcription Factor 9) and *aggrecan* (aggregating chondroitin sulfate proteoglycans) in the cells was determined by qPCR (Fig. 6).

Upregulation of *Akt-1* or *PI3K* was detected in the cells of most of the donors exposed to 18 J/cm^2. Compared with those of the other two groups, the 18 J/cm^2 groups in the No. 1, No. 5 and No. 6 samples were significantly greater, and most of the 4 J/cm^2 groups were not significantly different from the control group, except for Akt-1 in the No. 4 and PI3K in the No. 3 samples. Specifically, no significant differences were observed among the groups in the cells of No. 2 and No. 3 for *Akt-1* or No. 4 for *PI3K* (Fig. 6a,b). *Akt-1* and *PI3K* were confirmed as PBM-related signaling pathways. Given that *Ki67*, *Notch-1, TGF-β3, Col2A1, Sox9* and *Aggrecan* were upregulated in some of the donor cells in the 4 J/cm^2 group (Fig. 6c,d,e,f,g,h), it is possible that the genes or signaling pathways involved in the response of MeSCs to PBM are not limited to *Akt*/*PI3K*. It is also possible that the different response rates of the *Akt*/*PI3K* pathway in different cells led to the different levels of *Akt-1* and *PI3K* upregulation that we detected in different samples.

Ki67 and *Notch-1* are genes were associated with cell proliferation. As shown in Fig. 6c,d, in samples No. 1, No. 2, No. 3 and No. 5, *Ki67* and *Notch-1* were significantly greater in the 18 and 4 J/cm^2 groups than in the control group. There were also significant differences between the 4 J/cm^2 groups and the control groups. There was no significant difference between the groups in samples No. 4 and No. 6.

As chondrogenic-related genes, *TGF-β3*, *Col2A1*, *Sox9* and *Aggrecan* presented different levels of variation in different samples. *TGF-β3* was upregulated in the 18 J/cm^2 groups of all samples and in the 4 J/cm^2 group of one sample (No. 4). *Col2A1* was upregulated in the 18 J/cm^2 groups of No. 2, No. 5 and No. 6 and in the 4 J/cm^2 groups of No. 5 and No. 6. *Sox9* was upregulated in the 18 J/cm^2 groups in almost all the samples except for No. 3, but in the 4 J/cm^2 group, only No. 4 was upregulated. Among the 18 J/cm^2 samples, almost all samples except No. 5 were upregulated, but among the 4 J/cm^2 samples, only No. 1 was upregulated.

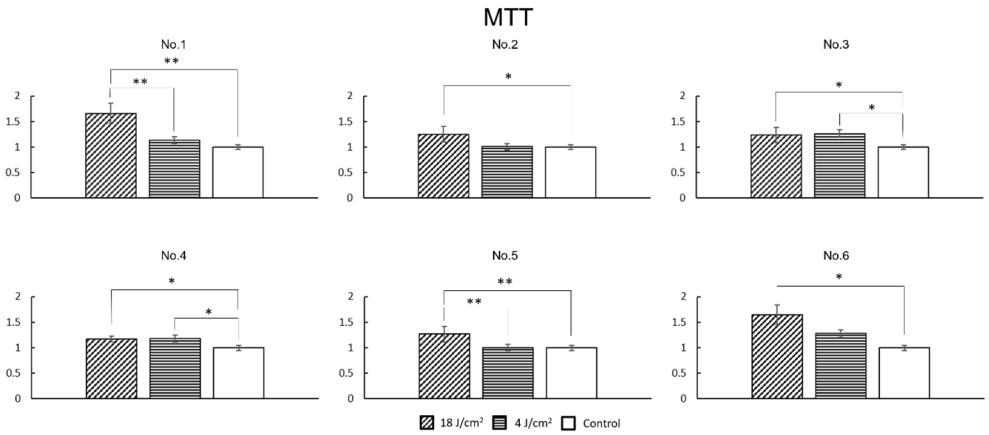

Figure 3. MeSCs were subjected to the MTT assay at 24 h after irradiation, with the absorbance at 570/630 nm. $n = 3$; $^*p < 0.05$, $^{**}p < 0.01$.

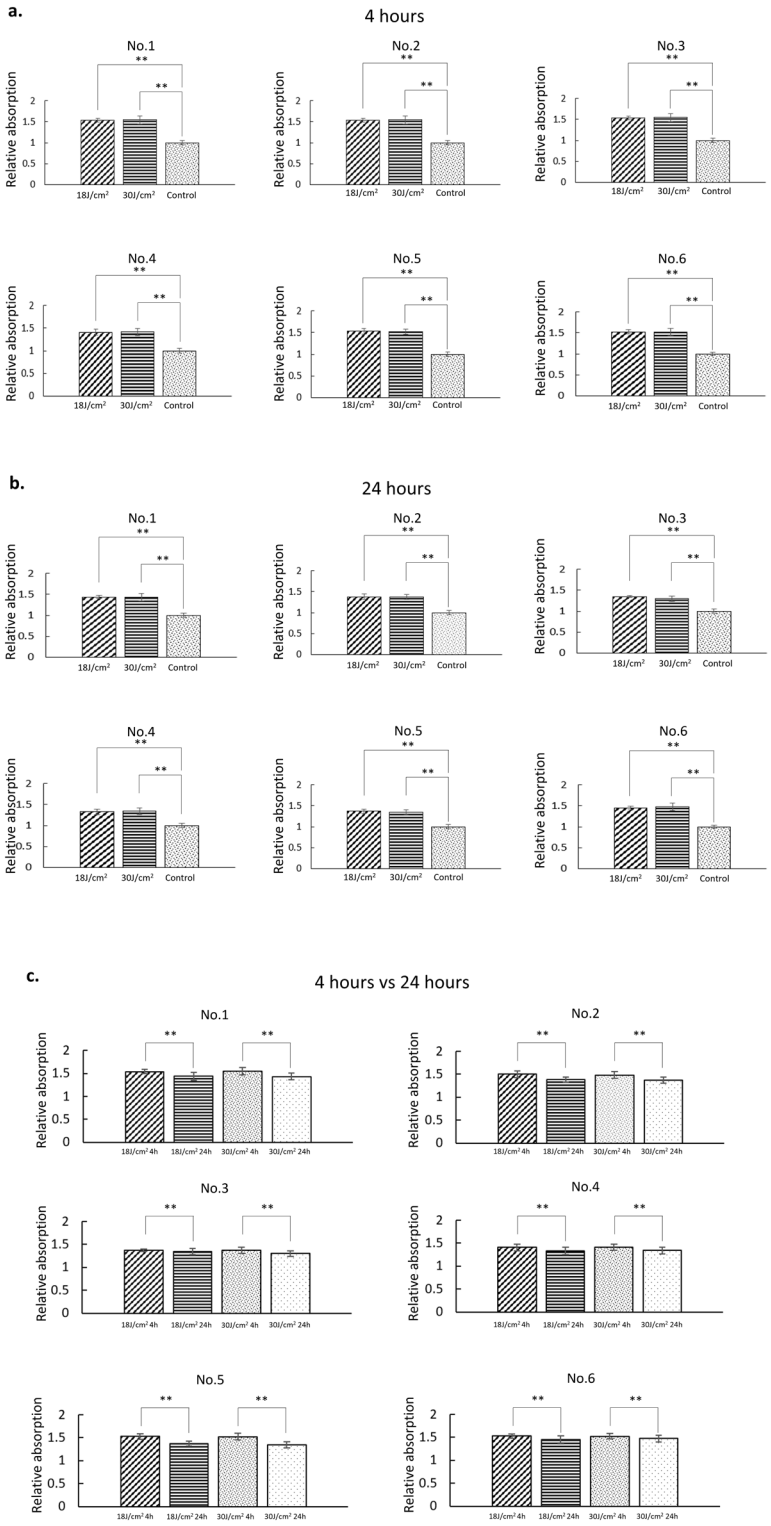

Figure 4. MeSCs were subjected to the MTT assay at 4 and 24 h after irradiation, at which point the absorbance at 570/630 nm was measured. (**a**) Four hours after irradiation, the MTT values of the 18 and 30 J/cm^2 groups were significantly greater than those of the control group; (**b**) Twenty-four hours after irradiation, the MTT values of the 18 and 30 J/cm^2 groups were significantly greater than those of the control group; (**c**) The MTT value at 4 h after irradiation was greater than that at 24 h. $n = 3$; $^*p < 0.05$, $^{**}p < 0.01$.

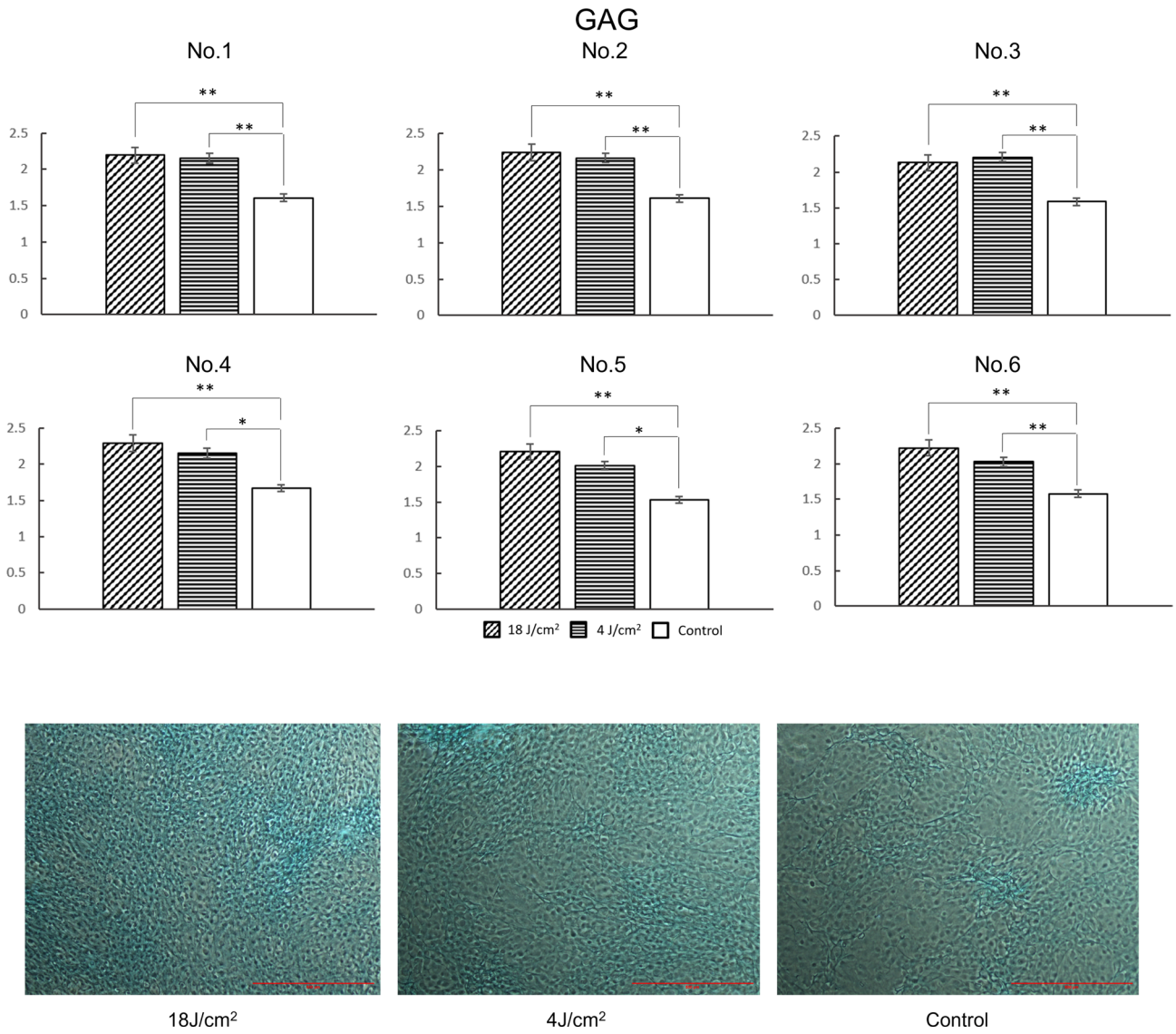

Figure 5. Comparison of the effects of the PBM at different power densities. DMMB assays were used to determine the production of GAGs in differentiated MeSCs. (**a**) The values in the 18 and 4 J/cm^2 groups were greater than those in the control group for all samples, but there was no significant difference between the 18 and 4 J/cm^2 groups. $n = 3$; $^*p < 0.05$, $^{**}p < 0.01$. (**b**) Alcian blue staining; scale bars = 500 μm.

RNA was extracted from irradiated cells from donor No. 1, and gene expression was detected via qPCR. *Akt-1*, *PI3K*, *Ki67*, *Notch-1*, *TGF-β3*, *Col2A1*, *Sox9* and *Aggrecan* were upregulated in most samples in the 18 J/cm^2 group and in a few samples in the 4 J/cm^2 group. $n = 3$; $^*p < 0.05$, $^{**}p < 0.01$.

The *PI3K*/*Akt*/*mTOR* signaling pathway is an important intracellular network that leads to cell proliferation. Several studies have shown that *Src* kinase increases the activity of *PI3K*[26]. At 8, 16, and 24 h, *Src* mRNA expression was 39.6%, 31.0%, and 27.9% greater than that in the control group; *PI3K* expression was 30.2%, 21.1%, and 20.9% greater than that in the control group; *Akt-1* expression was 45.2%, 36.2%, and 25.1% greater than that in the control group; and *mTOR* expression was 24.3%, 18.2%, and 12.3% greater than that in the control group. The *PI3K*/*Akt*/*GSK3β* signaling pathway plays a critical role in the regulation of cell growth and survival, with *GSK3β* facilitating apoptosis by activating transcription factors. At 8, 16, and 24 h, the level of *GSK3β* was 18.9%, 32.1%, and 18.7% lower than that in the control group, respectively (Fig. 7).

JNK, *p38*, *MAPK*, *JAK*, *Bax*, *Bcl*, *p21* and *p53* have also been reported to be involved in some of the signaling pathways associated with the effect of PBM on cells. Our results revealed no significant differences between the 18 J/cm^2 group and the control group at any time point (Fig. 7).

MeSCs from donor No. 1 were irradiated at 18 J/cm^2 one time, and the cells were harvested at 8, 16 and 24 h postirradiation. The RNA was also harvested from the control group at the same time points. Gene expression was detected via qPCR. The histograms show the multiples of the irradiated group compared with the control group. $n = 3$; $^*p < 0.05$, $^{**}p < 0.01$.

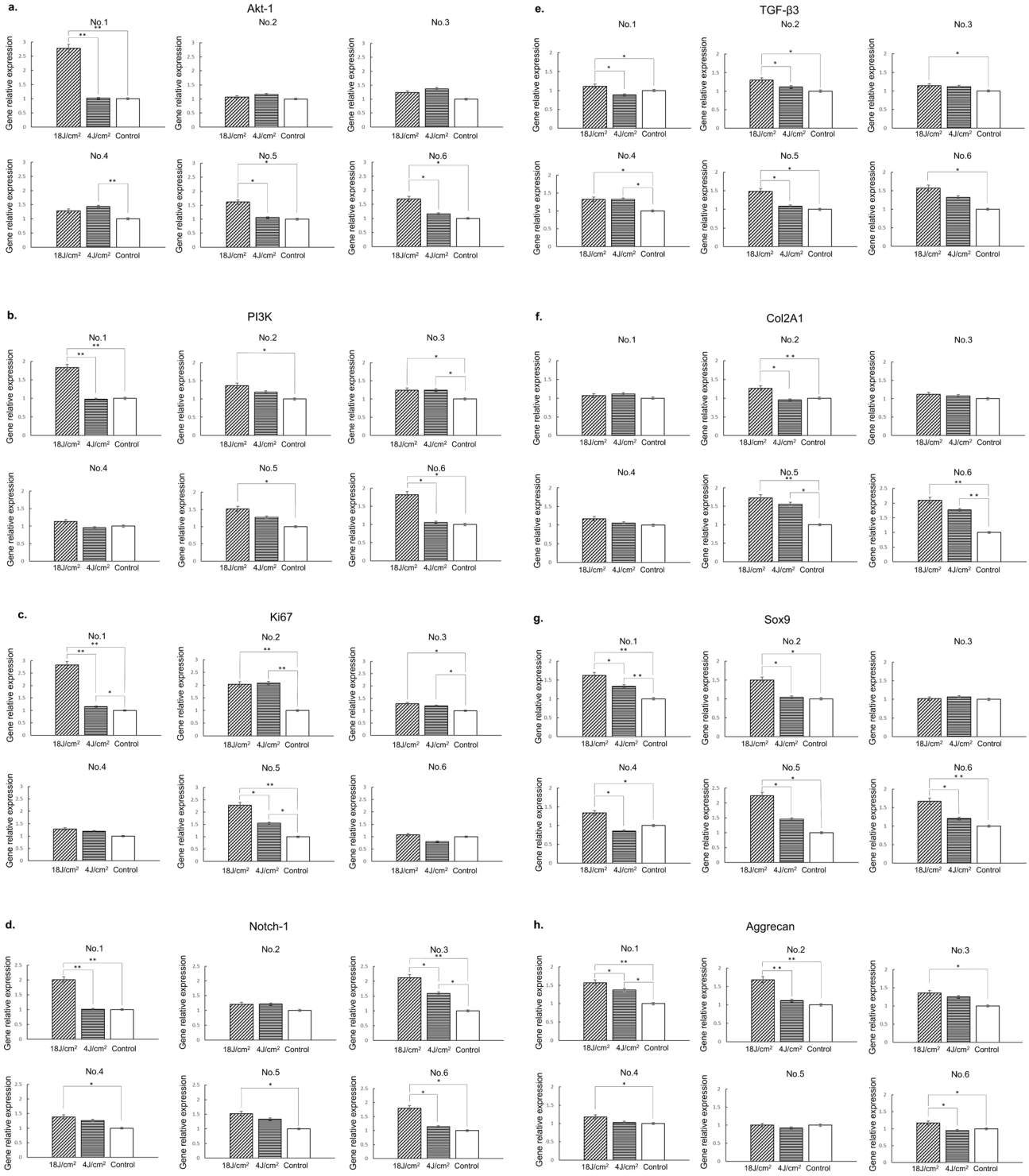

Figure 6. Gene expression results.

Discussion

Despite the positive results of the application of PBM to different MSCs[27], the relationship between the parameters of PBM and its effect on cells cannot yet be determined in detail and with precision due to the great variation in protocol design and results. For example, the optimal energy densities for MSCs used in previous studies were 1 J/cm^2[28], 8 J/cm^2[29] and 60 J/cm^2[30], whereas the optimal wavelengths for PBM studies were blue light (400–500 nm), red light (620–660 nm) and near-infrared light (800–980 nm)[13,31]. Since the effect of PBM on MeSCs has not been previously reported, we chose one of the more commonly reported wavelengths (660 nm) and selected three values (4 J/cm^2, 18 J/cm^2, and 30 J/cm^2) within the more common energy density range for a preliminary investigation.

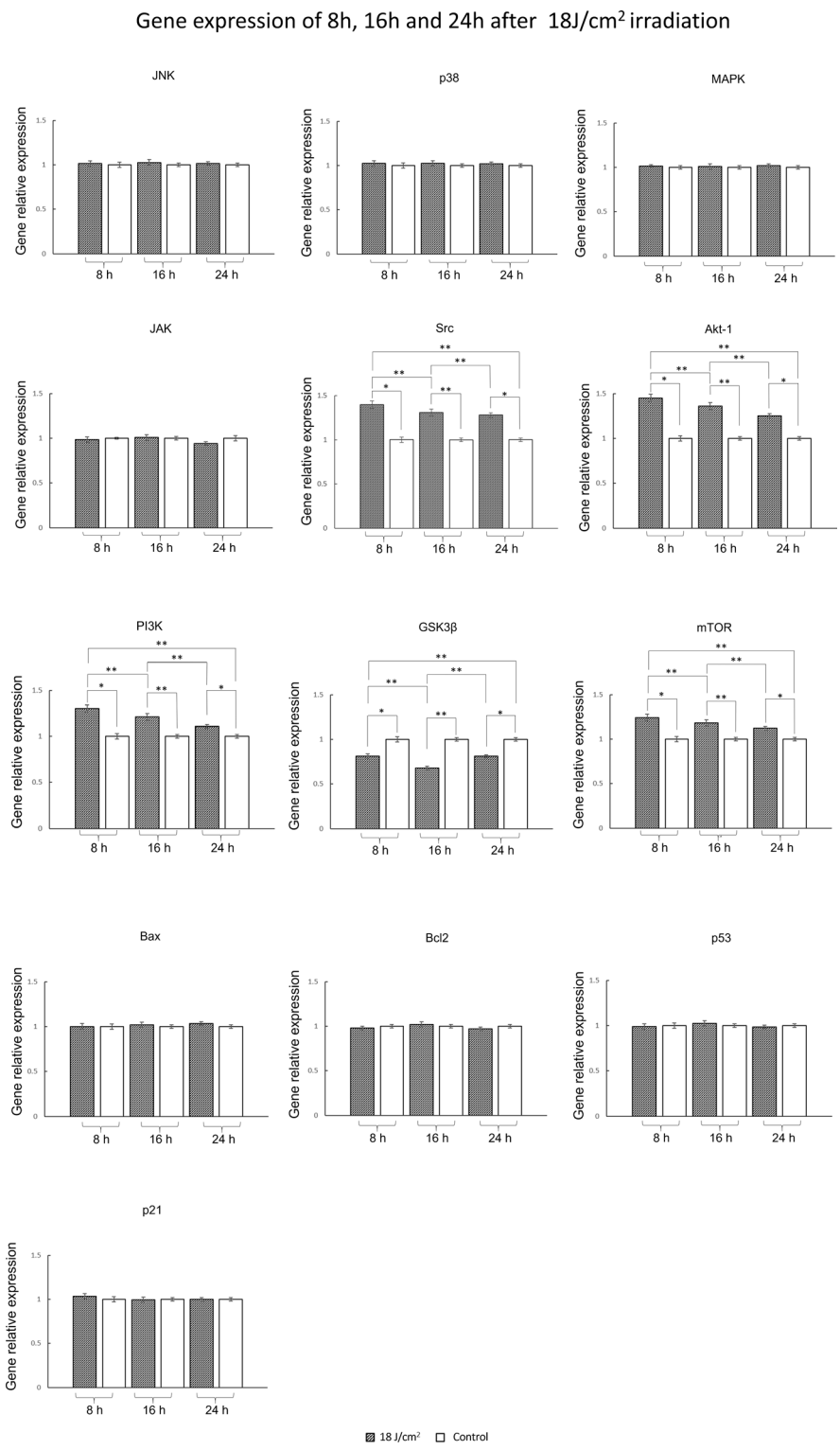

Figure 7. Gene expression results.

The primary concept regarding the mechanism of PBM in cells is that the photons emitted by PBM are absorbed by chromophores within the mitochondria, with the enzyme cytochrome c oxidase absorbing primarily red and infrared light[32]. The activation of the enzyme cytochrome c oxidase can enhance the functions of calcium ions, reactive oxygen species (ROS), ATP, nitric oxide (NO), and various other signaling molecules, thereby stimulating cellular activity[33,34].

Although there are many reports in the literature that PBM can promote the ability of MSCs to proliferate and differentiate, there are discrepancies in the conclusions reached by different studies, some of which

observed an element of uncertainty and failed to reveal the potential cause[14]. For example, between reports with similar research objectives, there are large differences in the effects obtained for the same energy density of irradiation[29,35–38]. In addition, cells treated with PBM in both 2D and 3D culture environments showed significant differences or even extreme polar changes in cell proliferation and differentiation[35].

In addition, some of the previous studies on the PBM effects on MSCs lacked an in-depth investigation of the related gene expression and molecular mechanisms. For example, in recent years, many studies on the differentiation ability of dental pulp stem cells have detected only changes in cell differentiation ability via specific staining but not in RNA and protein expression[19,20]; studies on the cartilage differentiation of bone marrow stem cells have detected only the expression of genes related to cartilage differentiation products but not the expression of genes upstream of the cartilage differentiation pathway, which is directly related to PBM[21]. In this novel study, we aimed to detect the effects of 660-nm PBM on promoting the proliferation, mitochondrial activity and chondrogenic differentiation potential of MeSCs and to explore the underlying molecular mechanisms by detecting gene expression changes.

In the present study, by testing the effects of 660-nm LED red light at different energy densities on MeSCs, we demonstrated that 660-nm LED PBM promotes the proliferation, mitochondrial activity, chondrogenic differentiation potential and related gene expression of MeSCs. NCPD and CPDT were used to evaluate the proliferation ability of MeSCs. Compared with that in the 4 J/cm^2 and control groups, the proliferation of passage 3 cells in the 18 J/cm^2 group was significantly greater (Fig. 2). DMMB assays revealed that the 18 J/cm^2 groups contained significantly more GAGs than the 4 J/cm^2 and control groups did after the induction of chondrogenic differentiation (Fig. 5). The MTT results following exposure to PBM revealed that all donor samples exposed to 18 J/cm^2 had significantly greater mitochondrial activity compared with the control samples, and only two samples presented greater mitochondrial activity when exposed to 4 J/cm^2 than the control samples (No. 3 and No. 4) (Fig. 4).

A comparison of the gene expression results revealed that No. 3 was the only sample with higher *PI3K* expression in the 4 J/cm^2 group than in the control group, and No. 4 was the only sample with higher *Akt-1* expression in the 4 J/cm^2 group than in the control group. The expression of most of the genes examined was significantly greater in the 18 J/cm^2 group than in the control group, and the expression of fewer genes was significantly greater in the 18 J/cm^2 groups than in the cells exposed to 4 J/cm^2 light irradiation (Fig. 6). The lower energy density (4 J/cm^2) slightly upregulated *Akt-1*, *PI3K*, *Ki67*, *Notch-1*, *TGF-β3*, *Col2A1*, *Sox9* and *Aggrecan* gene expression in a few donors and promoted chondrogenic differentiation ability in all of them, and increased mitochondrial activity was also observed in some samples. However, a lower energy density had no significant effect on promoting proliferation ability (Fig. 6).

Regarding cell proliferation and differentiation, *Akt-1* and *PI3K* play important roles in the effects of PBM[13]. As one of the most versatile kinase families, *Akt-1* is a key regulator of cell proliferation, metabolism and migration and can regulate the cell cycle and DNA damage checkpoint signaling[39]. In the downstream pathway of the tyrosine protein kinase receptor *(TPKR)* signaling pathway, *PI3K* phosphorylation plays an important role in cell proliferation[40]. By phosphorylating *Akt* and *PI3K*, low-level lasers activate eukaryotic translation initiation Factor 4E (*eIF4E)* through the phosphorylation of *mTOR* and promote cell proliferation and migration through the phosphorylation of *eIF4E*[41–43]. Our results revealed that *Akt-1* was significantly upregulated in the 18 J/cm^2 group (four samples) and in the 4 J/cm^2 group (one sample), and *PI3K* was significantly upregulated in the 18 J/cm^2 group (five samples) and in the 4 J/cm^2 group (one sample) (Fig. 6b). The changes in the expression of these two genes were correlated with changes in proliferation and chondrogenic differentiation (Figs. 2 and 4). There are two possible reasons for this result: (1) the *PI3K*/*Akt* pathway is not the only pathway by which PBM regulates the proliferation and differentiation of MeSCs, and (2) cells from different donor sources respond to PBM at different rates; thus, different gene expression differences were again observed at the same time point.

Based on these results, we further verified the signaling pathways involved in PBM reported in other articles[40,44]. In the cells from donor No. 1, *Akt-1* and *PI3K* gene expression was most highly upregulated. Since cells can continue to proliferate after PBM irradiation, most cells may not receive direct irradiation when they are examined for a longer period of time. When the PBM irradiates the cells multiple times, the number of times and the energy density of different cells directly irradiated by the PBM are inconsistent. Due to these factors and the lack of similar study protocols in previous studies for reference, we performed only one PBM irradiation and collected the cells at a short interval (8, 16 and 24 h) after irradiation to exclude the interference of the above factors for verification of signaling pathways.

The results revealed that *Src*, *PI3K*, *Akt*-1 and *mTOR* were upregulated in the PBM experimental cell group at 8, 16, and 24 h after irradiation compared with those in the control group, and the degree of upregulation decreased with time. However, *GSK3β* was significantly downregulated, with the most significant decrease observed at 16 h after irradiation. Some investigators have hypothesized that PBM causes a decrease in ROS in certain cells, which may activate the *Src* and *PI3K*/*Akt* signaling pathways[45]. Our results verified the existence of the same phenomenon in MeSCs and revealed that the effect of PBM on gene expression varied depending on the interval after irradiation.

Our results are in agreement with those of a previous study reporting that low-level laser irradiation resulted in the upregulation of genes related to the *Akt*/*PI3K*/*mTOR* pathway in rat bone marrow MSCs, and it was hypothesized that PBM may promote the proliferation of MSCs through this pathway[46]. The results revealed that the expression of the *Akt-1*, *Vdac-1*, and *Ptpn-6* genes was upregulated within 8 days after 635-nm low-level laser irradiation; however, the extent of upregulation varied with time (e.g., the expression of *Akt-1* showed an upward trend from 0 to 8 days after irradiation, whereas that of *Ptpn-6* peaked on the fourth day before declining)[46]. Because of the significant differences between our study and the experimental methods used in this report, it is not possible to provide a specific analysis or speculation regarding the cause of this discrepancy.

The upregulation of *mTOR* and downregulation of *GSK3β* are consistent with the results of previous studies on the effects of PBM on other cells and tissues[47]. To our knowledge, very few PBM studies on MSCs have directly detected changes in the gene expression of the *PI3K*/*Akt*/*mTOR* or *PI3K*/*Akt*/*GSK3β* pathway, and our results provide clearer evidence for the role of this pathway in the promotion of MSC proliferation and differentiation by PBM.

The results of other studies in other types of cells revealed that PBM with varying light wavelengths and energy densities could affect the gene expression of the JNK/*NF-κB*/*MMP-1*, *ERK1/2 MAPK/P38*, ΔΨm/ATP/cAMP/*JNK*/*AP-1*, *ERK1/2*/*MAPK*/*p38*, JNK/MAPK, and *JAK*/*STAT* pathways and may lead to changes in the expression of the *Bcl-2*, *Bax*, *p53*, and *p21* genes[15]. However, our experimental results revealed that the expression of the *JNK*, *p38*, *MAPK*, *JAK*, *Bcl-2*, *Bax*, *p53*, and *p21* genes did not significantly change; therefore, 660-nm light is believed to not exert cellular effects through the above pathways/genes.

High *Ki67* expression indicates that cells are proliferating rapidly[48]. *Notch-1* is a key receptor in the Notch signaling pathway and encodes an important member of the Notch family of proteins; overexpression of *Notch-1* promotes MSC proliferation, whereas inhibition of *Notch-1* expression decreases BMSC proliferation[49]. The qPCR results revealed that *Ki67* and *Notch-1* were significantly upregulated (Fig. 6c,d). However, only three of the samples exhibited simultaneous upregulation of both *Ki67* and *Notch-1*. These changes could be attributed to the variability of the donors. This phenomenon was also observed for *Akt-1*, *PI3K* and chondrogenic gene expression.

In the study of the ability of PBM to promote the chondrogenic differentiation potential of MSCs, numerous reports have shown that red light is the most desirable wavelength[50]. Studies on the effects of these wavelengths of light illumination on signaling pathways related to chondrogenic differentiation have focused mainly on the activity of genes such as *TGF-β1*, *TGF-β3*, *Wnt*, *Sox9* and *Col2A1*[10,42].

Our results revealed that 660-nm PBM promoted the chondrogenic differentiation of MeSCs by significantly increasing the expression of *TGF-β3* (Fig. 6e). However, no significant upregulation was detected for *Col2A1* in three samples, *Sox9* in one sample or *Aggrecan* in one sample (Fig. 6f,g,h). Thus, we could only confirm the preliminary effect of 660-nm PBM on the chondrogenic differentiation potential of MeSCs, and more in-depth studies are needed to investigate factors such as the state of the donor cells and the timing of changes in the relevant signaling pathways. Previous studies have also failed to investigate the effects of PBM on upstream and downstream gene expression changes in relevant pathways, which is a shortcoming of our current study.

Next, we investigated whether increasing the energy density to 30 J/cm^2 improved the mitochondrial activity of the cells. The MTT results revealed that mitochondrial activity was not improved compared with that in the cells exposed to 18 J/cm^2 (Fig. 4a,b). Other studies also reported similar results and revealed that exposure to higher energy density could instead lead to adverse effects[51]. Based on this result, we assume that the best energy density for the MeSC in 660-nm LED light is between 18 and 30 J/cm^2. Compared with those at 24 h, the cells tested at 4 h after irradiation presented greater mitochondrial activity. This result revealed that the effect of PBM on MeSCs decreased with time.

In this study, we focused on the application of a 660-nm LED PBM to stimulate MeSCs. Although our study did not explore the comparative effects of different wavelengths of red light or the differences between pulsed and continuous light, it provides a strong foundation for future investigations in these areas. In addition, existing research suggests that PBM above 30 J/cm^2 may enhance the differentiation of MSCs, suggesting the potential for further exploration beyond the energy densities examined in our study.

Nevertheless, this study revealed that the 660-nm LED PBM promoted the proliferative capacity and chondrogenic differentiation potential of MeSCs; even in older donor MeSCs, PBM promoted their proliferation and chondrogenic differentiation potential. This can be used as a pretreatment for cell therapy. In addition, red light has been shown to readily penetrate collagenous tissues or tissue-engineered materials; therefore, 660-nm LED PBM holds promise for the delivery of PBM into damaged menisci in arthroscopic surgical procedures to promote injury repair or as scaffold cells for meniscal tissue engineering. This method is inexpensive, minimally invasive, does not alter the genome of the cell culture, and selectively acts directly on the cells in the defect area due to the physical properties of the laser radiation.

Compared with other studies on the effects of PBM on MSCs[13,52], the present study more clearly demonstrated the effects of 660-nm LED light on the gene expression of the *PI3K/Akt/mTOR* and *PI3K/Akt/GSK3β* signaling pathways and revealed that the effects of PBM on mitochondrial activity and gene expression decreased with time. However, our study still had many limitations. Our multiple assays yielded different results in different samples, but we could not identify the detailed reasons for these differences. Although we detected differences in mRNA expression, we could not confirm these differences via protein expression assays. We examined changes in mitochondrial activity and gene expression only 8–24 h after exposure, which is too short a time period.

Conclusion

This study revealed the effects of 660-nm LED PBM on the proliferation, mitochondrial activity, chondrogenic differentiation ability and gene expression of MeSCs. The ability of the 660-nm LED PBM to promote MeSC proliferation may be related to the *PI3K/Akt/mTOR* and *PI3K/Akt/GSK3β* signaling pathways, whereas its ability to improve the chondrogenic differentiation ability of MeSCs may be related to the *TGF-β3*-related signaling pathways. This study provides a theoretical basis and preliminary reference data for PBM as a cell and processing tool for MeSC therapy and tissue engineering. In the future, it will be necessary to conduct more in-depth studies on the molecular mechanism of PBM and the optimal parameters for its action on MeSCs.

Data availability

The datasets generated and/or analyzed during the current study are available from the corresponding author upon reasonable request.

Received: 25 April 2024; Accepted: 14 August 2024
Published online: 26 August 2024

References

1. Luvsannyam, E., Jain, M. S., Leitao, A. R., Maikawa, N. & Leitao, A. E. Meniscus tear: Pathology, incidence, and management. *Cureus* **14**, e25121 (2022).
2. Luo, A. *et al.* Visual interpretable MRI fine grading of meniscus injury for intelligent assisted diagnosis and treatment. *npj Digit. Med.* **7**, 97 (2024).
3. Wiley, T. J. *et al.* Return to play following meniscal repair. *Clin. Sports Med.* **39**, 185–196 (2020).
4. Faucett, S. C. *et al.* Meniscus root repair vs meniscectomy or nonoperative management to prevent knee osteoarthritis after medial meniscus root tears: Clinical and economic effectiveness. *Am. J. Sports Med.* **47**, 762–769 (2019).
5. Suzuki, S. *et al.* Morphological changes in synovial mesenchymal stem cells during their adhesion to the meniscus. *Lab. Invest.* **100**, 916–927 (2020).
6. Ding, G., Du, J., Hu, X. & Ao, Y. Mesenchymal stem cells from different sources in meniscus repair and regeneration. *Front. Bioeng. Biotechnol.* **10**, 796367 (2022).
7. Shen, W. *et al.* Intra-articular injection of human meniscus stem/progenitor cells promotes meniscus regeneration and ameliorates osteoarthritis through stromal cell-derived factor-1/CXCR4-mediated homing. *Stem Cells Transl. Med.* **3**, 387–394 (2014).
8. Korpershoek, J. V. *et al.* Selection of highly proliferative and multipotent meniscus progenitors through differential adhesion to fibronectin: A novel approach in meniscus tissue engineering. *Int. J. Mol. Sci.* **22**, 8614 (2021).
9. Ding, Z. & Huang, H. Mesenchymal stem cells in rabbit meniscus and bone marrow exhibit a similar feature but a heterogeneous multi-differentiation potential: Superiority of meniscus as a cell source for meniscus repair evolutionary developmental biology and morphology. *BMC Musculoskelet. Disord.* **16**, 1–14 (2015).
10. Bunch, J. Photobiomodulation (therapeutic lasers): An update and review of current literature. *Vet. Clin. North Am. Small Anim. Pract.* **53**, 783–799 (2023).
11. Abbara, M. T. *et al.* Can diode laser 810 nm decrease post endodontic pain in patients with asymptomatic necrotic maxillary incisors? A four-arm randomized controlled trial. *BDJ Open* **10**, 23 (2024).
12. Hu, X. *et al.* Spinal cord injury: Molecular mechanisms and therapeutic interventions. *Signal Transduct. Target. Ther.* **8**, 245 (2023).
13. Mohamad, S. A., Milward, M. R., Hadis, M. A., Kuehne, S. A. & Cooper, P. R. Photobiomodulation of mineralisation in mesenchymal stem cells. *Photochem. Photobiol. Sci. Off. J. Eur. Photochem. Assoc. Eur. Soc. Photobiol.* **20**, 699–714 (2021).
14. Khorsandi, K., Hosseinzadeh, R., Abrahamse, H. & Fekrazad, R. Biological responses of stem cells to photobiomodulation therapy. *Curr. Stem Cell Res. Ther.* **15**, 400–413 (2020).
15. Ahrabi, B. *et al.* The effect of photobiomodulation therapy on the differentiation, proliferation, and migration of the mesenchymal stem cell: A review. *J. lasers Med. Sci.* **10**, S96–S103 (2019).
16. Firouz, B. *et al.* Testing the effects of photobiomodulation on angiogenesis in a newly established CAM burn wound model. *Sci. Rep.* **13**, 22985 (2023).
17. Muneekaew, S., Wang, M.-J. & Chen, S. Control of stem cell differentiation by using extrinsic photobiomodulation in conjunction with cell adhesion pattern. *Sci. Rep.* **12**, 1812 (2022).
18. Yoon, S. R., Chang, S.-Y., Lee, M. Y. & Ahn, J.-C. Effects of 660-nm LED photobiomodulation on drebrin expression pattern and astrocyte migration. *Sci. Rep.* **13**, 6220 (2023).
19. Zaccara, I. M. *et al.* Photobiomodulation therapy improves multilineage differentiation of dental pulp stem cells in three-dimensional culture model. *J. Biomed. Opt.* **23**, 1 (2018).
20. Dawoud, L. E., Hegazy, E. M., Galhom, R. A. & Youssef, M. M. Photobiomodulation therapy upregulates the growth kinetics and multilineage differentiation potential of human dental pulp stem cells—An in vitro Study. *Lasers Med. Sci.* **37**, 1993–2003 (2022).
21. Fekrazad, R. *et al.* Photobiomodulation with single and combination laser wavelengths on bone marrow mesenchymal stem cells: Proliferation and differentiation to bone or cartilage. *Lasers Med. Sci.* **34**, 115–126 (2019).
22. Verdonk, P. C. M. *et al.* Characterisation of human knee meniscus cell phenotype. *Osteoarthr. Cartil.* **13**, 548–560 (2005).
23. Chahla, J. *et al.* Assessing the resident progenitor cell population and the vascularity of the adult human meniscus. *Arthroscopy* **37**, 252–265 (2021).
24. Lee, J., Jang, S., Kwon, J., Oh, T. I. & Lee, E. Comparative evaluation of synovial multipotent stem cells and meniscal chondrocytes for capability of fibrocartilage reconstruction. *Cartilage* **13**, 980S-990S (2021).
25. Yang, Y.-H.K., Ogando, C. R., Wang See, C., Chang, T.-Y. & Barabino, G. A. Changes in phenotype and differentiation potential of human mesenchymal stem cells aging in vitro. *Stem Cell Res. Ther.* **9**, 131 (2018).
26. Beadnell, T. C. *et al.* Src-mediated regulation of the PI3K pathway in advanced papillary and anaplastic thyroid cancer. *Oncogenesis* **7**, 23 (2018).
27. Eroglu, B. *et al.* Photobiomodulation has rejuvenating effects on aged bone marrow mesenchymal stem cells. *Sci. Rep.* **11**, 13067 (2021).
28. Zare, F., Bayat, M., Aliaghaei, A. & Piryaei, A. Photobiomodulation therapy compensate the impairments of diabetic bone marrow mesenchymal stem cells. *Lasers Med. Sci.* **35**, 547–556 (2020).
29. Wang, L. *et al.* Low-level laser irradiation modulates the proliferation and the osteogenic differentiation of bone marrow mesenchymal stem cells under healthy and inflammatory condition. *Lasers Med. Sci.* **34**, 169–178 (2019).
30. Amaroli, A. *et al.* The effects of photobiomodulation of 808 nm diode laser therapy at higher fluence on the in vitro osteogenic differentiation of bone marrow stromal cells. *Front. Physiol.* **9**, 123 (2018).
31. Li, H. *et al.* The implication of blue light-emitting diode on mesenchymal stem cells: A systematic review. *Lasers Med. Sci.* **38**, 267 (2023).
32. Wang, Y., Huang, Y. Y., Wang, Y., Lyu, P. & Hamblin, M. R. Photobiomodulation (blue and green light) encourages osteoblastic-differentiation of human adipose-derived stem cells: Role of intracellular calcium and light-gated ion channels. *Sci. Rep.* **6**, 1–9 (2016).
33. Soliman, J., Elsanadi, R., Messele, F. & Kelly, K. M. The effect of combined red, blue, and near-infrared light-emitting diode (LED) photobiomodulation therapy on speed of wound healing after superficial ablative fractional resurfacing. *Lasers Med. Sci.* **39**, 94 (2024).
34. Lim, L. Traumatic brain injury recovery with photobiomodulation: Cellular mechanisms, clinical evidence, and future potential. *Cells* **13**, 385 (2024).
35. Schneider, C. *et al.* The impact of photobiomodulation on the chondrogenic potential of adipose-derived stromal/stem cells. *J. Photochem. Photobiol. B.* **221**, 112243 (2021).
36. Liao, X. *et al.* Preconditioning with low-level laser irradiation enhances the therapeutic potential of human adipose-derived stem cells in a mouse model of photoaged skin. *Photochem. Photobiol.* **94**, 780–790 (2018).
37. Bonvicini, J. F. S. *et al.* Specific parameters of infrared LED irradiation promote the inhibition of oxidative stress in dental pulp cells. *Arch. Oral Biol.* **131**, 105273 (2021).
38. Kulkarni, S., Meer, M. & George, R. The effect of photobiomodulation on human dental pulp-derived stem cells: Systematic review. *Lasers Med. Sci.* **35**, 1889–1897 (2020).

39. Deng, Z., Qing, Q. & Huang, B. A bibliometric analysis of the application of the PI3K-AKT-mTOR signaling pathway in cancer. *Naunyn. Schmiedebergs. Arch. Pharmacol.* https://doi.org/10.1007/s00210-024-03112-9 (2024).
40. El Gammal, Z. H., Zaher, A. M. & El-Badri, N. Effect of low-level laser-treated mesenchymal stem cells on myocardial infarction. *Lasers Med. Sci.* **32**, 1637–1646 (2017).
41. Leyane, T. S., Jere, S. W. & Houreld, N. N. Cellular signalling and photobiomodulation in chronic wound repair. *Int. J. Mol. Sci.* **22**, 11223 (2021).
42. Tian, T., Wang, Z., Chen, L., Xu, W. & Wu, B. Photobiomodulation activates undifferentiated macrophages and promotes M1/M2 macrophage polarization via PI3K/AKT/mTOR signaling pathway. *Lasers Med. Sci.* **38**, 86 (2023).
43. Benichou, E. *et al.* The transcription factor ChREBP Orchestrates liver carcinogenesis by coordinating the PI3K/AKT signaling and cancer metabolism. *Nat. Commun.* **15**, 1879 (2024).
44. Fekrazad, R., Asefi, S., Allahdadi, M. & Kalhori, K. A. M. Effect of photobiomodulation on mesenchymal stem cells. *Photomed. Laser Surg.* **34**, 533–542 (2016).
45. Rajendran, N. K., Houreld, N. N. & Abrahamse, H. Photobiomodulation reduces oxidative stress in diabetic wounded fibroblast cells by inhibiting the FOXO1 signaling pathway. *J. Cell Commun. Signal.* **15**, 195–206 (2021).
46. Wu, Y. *et al.* Effects of low-level laser irradiation on mesenchymal stem cell proliferation: A microarray analysis. *Lasers Med. Sci.* **27**, 509–519 (2012).
47. Jere, S. W., Houreld, N. N. & Abrahamse, H. Role of the PI3K/AKT (mTOR and GSK3β) signalling pathway and photobiomodulation in diabetic wound healing. *Cytokine Growth Factor Rev.* **50**, 52–59 (2019).
48. Wang, J. *et al.* Effects of different KRAS mutants and Ki67 expression on diagnosis and prognosis in lung adenocarcinoma. *Sci. Rep.* **14**, 4085 (2024).
49. He, Y. & Zou, L. Notch-1 inhibition reduces proliferation and promotes osteogenic differentiation of bone marrow mesenchymal stem cells. *Exp. Ther. Med.* **18**, 1884–1890 (2019).
50. Bozhokin, M. S. *et al.* Low-intensity photobiomodulation at 632.8 nm increases tgfβ3, col2a1, and sox9 gene expression in rat bone marrow mesenchymal stem cells in vitro. *Lasers Med. Sci.* **37**, 435–441 (2022).
51. de Freitas, L. F. & Hamblin, M. R. Proposed mechanisms of photobiomodulation or low-level light therapy. *IEEE J. Sel. Top. Quantum Electron.* **22**, 7000417 (2016).
52. Amaroli, A. *et al.* Steering the multipotent mesenchymal cells towards an anti-inflammatory and osteogenic bias via photobiomodulation therapy: How to kill two birds with one stone. *J. Tissue Eng.* **13**, 20417314221110190 (2022).

Author contributions

T.JB conceptualization; methodology; formal analysis; investigation; writing-original draft; data curation; project administration; funding acquisition. S.K.S. conceptualization; resources. S.R. resources. R.R. resources. W.XY. Funding acquisition. Y.YY. Funding acquisition. W.JJ Funding acquisition. M.P.L. conceptualization; writing-review and editing; data curation; project administration; funding acquisition.

Funding

This research was funded by the GP-IPS grant of Universiti Putra Malaysia (GP-IPS/2022/9718000).

Competing interests

The authors declare no competing interests.

Additional information

Correspondence and requests for materials should be addressed to J.T. or P.L.M.

Reprints and permissions information is available at www.nature.com/reprints.

Publisher's note Springer Nature remains neutral with regard to jurisdictional claims in published maps and institutional affiliations.